

# **Scanning acoustic microscopy. A possibility of application in investigation of optical glasses and fibres\***

A. GADOMSKI

Institute of Physics, Technical University of Wrocław, Wybrzeże Wyspiańskiego 27, 50-370 Wrocław, Poland.

S. BOSECK

University of Bremen, FRG.

The theory of the imaging process in a scanning acoustic microscope (SAM) is briefly presented. It is done by comparison with a scanning optical microscope (SOM), type 2. Under distinct condition, the SAM works similarly to a SOM, type 2, but it can also utilize an interference phenomenon in imaging process. SAM is very sensitive to surface topography, while good contrast in the image is possible to achieve also when the interference phenomenon does not take place. Next, the results of the measurements of the optical glasses and waveguide are presented, which indicate that there are technological processes applied in optical guide manufacturing which change simultaneously the optical and mechanical properties of the material processed.

## **1. Introduction**

The intention of this paper is to present the imaging properties and possibilities of SAM from the point of view of its application to investigation of optical glasses and elements to examine their quality and as a research tool to study their technology.

The purpose of Section 2 is to introduce briefly the readers into the present state of acoustic microscopy and to present the possibilities and confinements of this new nondestructive technique. In the next chapter, our attention is focused on the reflection version of SAM, the version which is utilized currently by the authors. All other chapters are also confined to reflection SAM. In Section 3 some unique properties of SAM, which distinguish it from the optical microscope, are described. Section 4 considers the imaging properties of SAM in comparison to its equivalent in the optical case SOM, type 2. Section 4.1 presents the imaging process in scanning mode of SAM when the ultrasonic beam focused by the ultrasonic lens is only reflected from the sample without excitation of surface waves. Section 4.2 deals with

---

\* Supported by Deutsche Forschungsgemeinschaft Bonn (DFG) Bo499/5-1. Part of Ph. D. (A.G.).

the imaging process when the part of the ultrasonic beam is transformed into the surface waves. Section 4.3 discusses the SAM operating in nonscanning mode when acoustical material signature is measured. The examples of the first of applying the SAM to investigation of the optical glasses and fibres are presented in Sect. 5. The results of the discussion and measurements are summarized in Sect. 6. The Appendix briefly explains the following terms: surface wave, leaky surface wave and the problem of dispersion in acoustic microscopy.

## 2. State-of-the-art of the scanning acoustic microscopy

There are two types of SAM: the transmission and the reflection. These both kinds of SAM are examples of general scanning microscope, type 2. The imaging properties of this type of scanning microscope, as exemplified by a SOM, type 2 (transmission and reflection version), were investigated by SHEPPARD and WILSON [1], [2] while similar calculations for the transmission SAM were published by LEMONS [3]. In the transmission version (Fig. 1), the ultrasonic beam passes through the object placed between

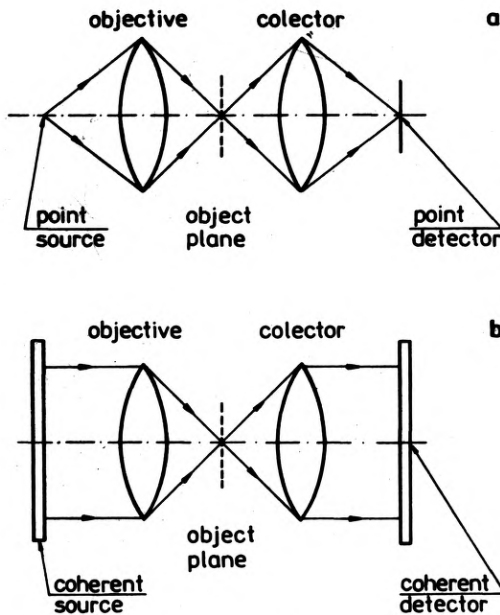


Fig. 1. Scanning microscopes: a – scanning optical microscope (SOM), type 2, and b – scanning acoustic microscope (SAM)

the objective and collector. Since SAM as a scanning microscope of type 2 has a sharply defined depth of field, a thin layer cut out from the interior of a thick specimen may be observed. In the transmission mode, it is especially suitable for investigation of the samples of acoustic impedance and attenuation comparable to those of water, i.e., for biological specimens. The reflection version is more promising to the investigation of the samples of high acoustical impedance and attenuation, i.e., the solid materials. In this version, the same lens plays the role of both objective and collector.

The ultrasonic picture as an image of mechanical properties in microscopic scale is an important supplement of optical image and offers unexpected possibilities. In the reflection microscopy, the elastic properties such as, for example, reflectance function, ultrasonic velocities, attenuation are imaged. Usually, all of those parameters influence the image and care must be taken in the course of its interpretation. In the picture of polycrystalline materials the grain structure is visible because of mechanical anisotropy [4]. The contrast distribution of plastically deformed area is primarily the image of ultrasonic attenuation [5], [6]. When there are simple surface or subsurface cracks in the field of view, they are also visible when their dimensions are several times smaller than the ultrasonic wavelength [5]. In the reflection image of the solid specimen, which has acoustic impedance much higher than that of water, there is primarily the piece of information on the surface topography, and reflection SAM is very sensitive to its topography.

The acoustic lens focuses the ultrasonic beam nearly to diffraction limit. The resolving power is primarily confined by the applied frequency, while the increase in the latter causes the increase in the resolution power. Unfortunately, the application of higher frequencies is restricted due to the attenuation of coupling medium and specimen. For example, the water heated up to 333 K as a coupling fluid allows the application of the operating frequency up to 2 GHz which gives the resolution about 0.5  $\mu\text{m}$ . The utilization of nonlinear properties of the coupling liquid was proposed to overcome this confinement. The generation of harmonics enables the improvement of the resolution of the microscope by, at least, a factor of 1.4 [7]. As an ultimate solution, the cryogenic acoustic microscope was applied with the superfluid helium as the coupling medium. This medium theoretically allows the investigation at the wavelength as short as 0.001  $\mu\text{m}$  (sound velocity of helium at 0.1 K is equal to 238 m/s and attenuation at 1 GHz is equal to 0.04 dB/mm) [7]. In the case of the cryogenic SAM, operating with 8 GHz frequency the resolution of micrographs obtained was better than 0.025  $\mu\text{m}$  [8]. At this level, the cryogenic acoustic microscopy as a research tool may offer an alternative to the electron microscopy. In contrast to the high energy electronic beam required for high resolution micrographs, the ultrasonic beam has not destructive properties. When the integrated circuits are investigated, the image from cryogenic acoustic microscope contains much more details and provides the pictures of resolution comparable to those of the scanning electron microscope [7], [9]. The acoustic impedance of the superfluid helium is extremely small and the contrast in the helium acoustic microscope is caused by topographical features.

The reflection SAM enables not only visualization but also the measurement of the mechanical parameters on the microscopic scale. The basis of this measurement is the registration of a  $V(z)$  function, the function describing the variation of the acoustic lens output signal when the specimen-lens distance is altered. The recovery of the reflectance function of the unknown object is possible from the  $V(z)$  function, also when the SAM delivers only the modulus of this function [10], [11]. The surface wave velocities and attenuation may be also extracted from this function [12], [13]. The measurements of the dispersive surface wave (see Appendix) enables calculation

of the thickness of the layer when the dispersion is caused by propagation of the surface waves on the interface between layered media. So, the SAM can be used as a thickness micrometer. On the other hand, the attenuation coefficient is the source of information about the quality of the surface on which the surface wave propagates [14]. It is also influenced by nanometer deficiencies [15]. Beside spherical, also cylindrical lenses with ultrasonic focus in the shape of the straight line are applied. The  $V(z)$  function measured with the cylindric focus using different orientations of the lens to the sample delivers information about its anisotropy [16].

### 3. General principle

The reflection scanning acoustic microscope is an important analytical tool currently developed for nondestructive testing of materials. The scheme of a SAM is illustrated in Fig. 2. The central part of it is an acoustic lens, a sapphire rod cut along C-axis

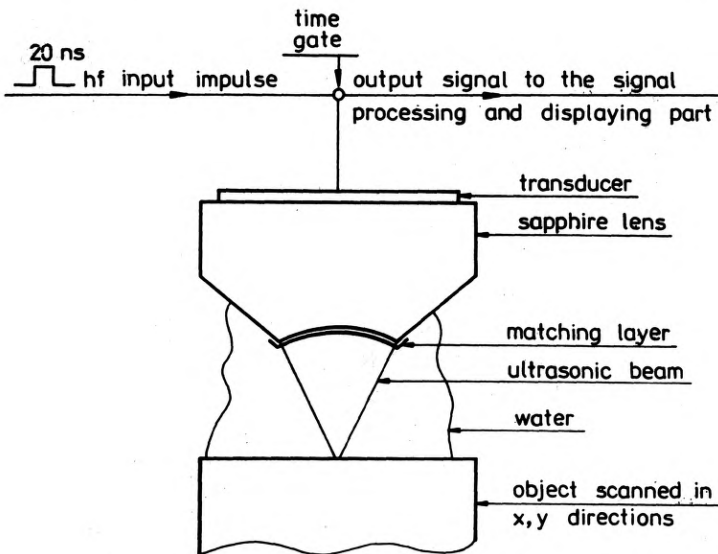


Fig. 2. Geometry of the imaging part of the SAM

with concave spherical surface on the front and plane surface with a piezoelectric transducer on the back side. The method developed by LEMONS and QATE [3] is as follows. A piezoelectric transducer is fed by the appropriate radio-frequency signal and generates the ultrasonic wave of the same frequency. The focus of the acoustic lens is then scanned in a raster pattern over a specimen with the amplitude of reflected echo being registered at each position. In this way a complete image is built up. Usually, time about 10 s is required to built up the whole image containing  $1024 \times 1024$  pixels. Under scanning mode SAM images the spatial distribution of the due mechanical properties. SAM may also work in a nonscanning mode. In this case, the acoustic lens is moved toward the specimen and the output voltage signal –  $V(z)$

function is registered. The nonscanning mode enables measurement of the acoustical properties on microscopic scale.

### **Unique properties**

In the case of SAM, the carrier of information is an ultrasonic wave. This wave propagates through the areas of highly different mechanical parameters, such as: ultrasonic lens, coupling medium, investigated specimen. Sapphire, the usual material of acoustic lenses, is characterized by the ultrasonic velocity being 7.4 times greater than that in water, which is usually applied as a coupling medium. It makes possible the application of the single surface as a microscopic objective of very good imaging properties. The negative consequence is the high impedance mismatch which requires the application of the quarter wavelength matching layer between the lens and coupling medium [17]. An acoustic lens generates a longitudinal convergent beam. If the aperture angle of this beam is smaller than the critical angle (Appendix), then both longitudinal and shear focuses with phase accordance can be generated inside a probe. When the aperture angle of the beam is greater than the critical angle, then leaky surface wave, leaky surface-skimming longitudinal, leaky Lamb waves, leaky pseudosurface waves and harmonics model of leaky surface waves can be excited on the liquid-solid interface. In the SAM imaging, first type of those waves is more significant than the others.

When an inward structure of a solid specimen is investigated by SAM, another difficulty appears. For the solid materials with ultrasonic velocity several times greater than this in water, the critical angle for total internal reflection and high impedance mismatch are present. In consequence, only a small part of the energy of the ultrasonic beam focused in water is transmitted into such materials. The ultrasonic beam, which is convergent nearly to the diffraction limit in water, loses this property inside the solid specimen.

The ultrasonic beam propagating through the lens, liquid and specimen is highly attenuated. The time gate (Fig. 2) is then necessary to separate the echo reflected at the specimen from the other echos (for example, those produced inside the lens). Thus, SAM must work in impulse mode – ultrasonic illumination is anharmonic. The duration of the impulse finite (about 20 ns) and the time resolution decreases. The attenuation confines also the depth of penetration which decreases rapidly with increasing operating frequency. When the operating frequency is about 2 GHz and water as a coupling fluid is applied, the resolving power is comparable to that of optical microscopy.

## **4. Imaging properties**

It is possible to distinguish several submodes under scanning mode. For a given acoustic lens this classification is based on the mechanical properties of the sample. In the case of the materials characterized by the critical angle greater than the aperture semi-angle of the lens, the surface waves are not generated and a SAM works as a pure reflection microscope (like SOM, type 2). If the specimen has the

acoustical impedance comparable to that of water, it is possible to observe structures under the surface of the probe [18]. This pure reflection mode enables practical utilization of the ability of ultrasonic waves to penetrate the interior of the opaque materials. The contrast distribution in the ultrasonic image of the surface or subsurface structure is primary conditioned by its reflectance function, topography or both of them.

When the probe has so high ultrasonic velocity that the applied lens can excite surface waves (the critical angle smaller than aperture semi-angle), and when also SAM operates with frequency greater than 1 GHz, we get first of all the information about the specimen surface and its nearest surrounding. Under such conditions, it is possible to consider SAM as an interference microscope.

#### 4.1. SAM as a pure reflection microscope

Considering imaging properties of the SAM, it is useful to refer to scanning microscopy, especially to the confocal scanning optical microscope, type 2. It was shown [1]–[3] that both the microscopes (SOM, type 2, and SAM) from the imaging point of view have similar properties and an acoustical (optical) arrangement (Fig. 1). This analogy is valid on the assumption that our SAM displays the complex amplitude detected by transducer which means in our case that the transfer function of both microscopes depends in the same way on the set-up parameters. In the SAM and SOM, type 2, the coherent source and detector are applied. In the case of SAM, the detector is amplitude-sensitive and has the extended integrating area. The transfer function  $C$  of SAM is the convolution of the pupils functions  $P_1$  and  $P_2$  and is given by the following formula [3], [19]:

$$C = P_1 * P_2$$

where:  $P_1, P_2$  – pupil functions of the acoustic lens for the out- (objective) and incoming (collector) ultrasonic beams, respectively; \* denotes convolution.

The SAM has coherent point imaging but its transfer function looks like that for an incoherent microscope [2], [20]. It was shown by LEMONS and QUATE [3] that if one assumes the aberration-free acoustic lens ( $P_1$  and  $P_2$  real) and identity of those functions ( $P_1 = P_2$ ), then this common transfer function is the same as for incoherent conventional microscope and SOM, type 1, i.e.,

$$C = P_1 * P_2^*,$$

( $P_1$  – pupil function of the objective of the conventional microscope or SOM, type 1). When the sample is positioned in the ultrasonic focus and the lens has a small aperture, then the assumption  $P_1 = P_2 = P = P^*$  is a permitted approximation. This results in small spherical aberration [3] and complex  $P_1, P_2$ . Defocusing gives also contribution to the imaginary part of the pupil functions. Different conditions of transmission of the ultrasonic beam to the coupling medium and back to the sapphire lens cause the pupil functions  $P_1, P_2$  to become unequal. Summing up, the functions  $P_1, P_2$  are generally different, complex and their imaginary part increases with defocusing. The complex pupil functions result in a complex optical transfer

function (OTF). Large amount of defocusing is available and, in consequence, the imaginary part of the resulting optical transfer function arises primarily when SAM is defocused. The imaginary part of the OTF is responsible for imaging of the phase detail of the object [21]. When  $P_1$  and  $P_2$  are complex, the amplitude and phase images are present in the same time. The modulus of the OTF increases in the course of defocusing to reach its maximum for the spatial frequency greater than zero [19]–[21]. Since the spherical aberration [3] of the acoustic lens is negligible, the amplitude image predominates when the object is in ultrasonic focus and the SAM images the spatial distribution of the modulus of the reflectance function. For most materials, this modulus change from 0.70 (glass) to 1.0 and at in-focus position a weak contrast is reached. Small amount of defocusing may cause an increase in the average contrast. In this place, it should be underlined that when the interface between the coupling medium and the specimen surface is observed, only a small amount of defocusing is possible because the SAM as a confocal microscope has a restricted depth of field [19], [22] and in the course of defocusing the output signal and the signal-to-noise ratio decrease rapidly and the output signal falls down to zero at a distance of about few micrometers. This phenomenon is illustrated by  $V(z)$  curve when the surface waves are not excited, Fig. 3 (the  $V(z)$  function without interference oscillation). Summarizing, when there is no surface wave excitation and the surface investigated is in the ultrasonic focus, the modulus of the reflectance function is to be imaged. The phase image appears together with defocusing. The analogy between SOM, type 2, and SAM may be utilized when SAM works in a pure reflection mode. The problem to solve is the extension of described [2], [3], [19], [20] theory, to include the case when the surface waves are excited.

One remark should be made. The images of the object points are completely separated. The transducer produces the next scanning probe after collecting the echo from the former point. In this sense, there is no coherence between scanning points. When comparing the diameter of the scanning spot with the scanning step, then one comes to conclusion that the difference between two different scanning areas is most often not greater than a few percents. In this sense, it is possible to speak about oversampling [23]. If a great change of the mechanical properties takes place within the scanning probe, which is common when the lens is defocused, there is still coherence between the scanning points but, of course, there exists also some coherence between points of the object investigated. Then the returning echo, reflected from the different part of the scanning probe, can interfere positively or negatively in the plane of the transducer, producing the "halo" effect. This effect may be so strong that the real structure of the sample disappears in the image [24].

The  $V(z)$  curve, when the surface waves are not excited, may be utilized to image the surface structure without excitation of the surface wave, i. e., to image the surface topography. The experiment was done for a gold probe polished with diamond past,  $3\mu\text{m}$  (Fig. 4). The conclusion is that the micrometer surface structure is visible without excitation of surface waves and SAM is very sensitive to the surface topography.

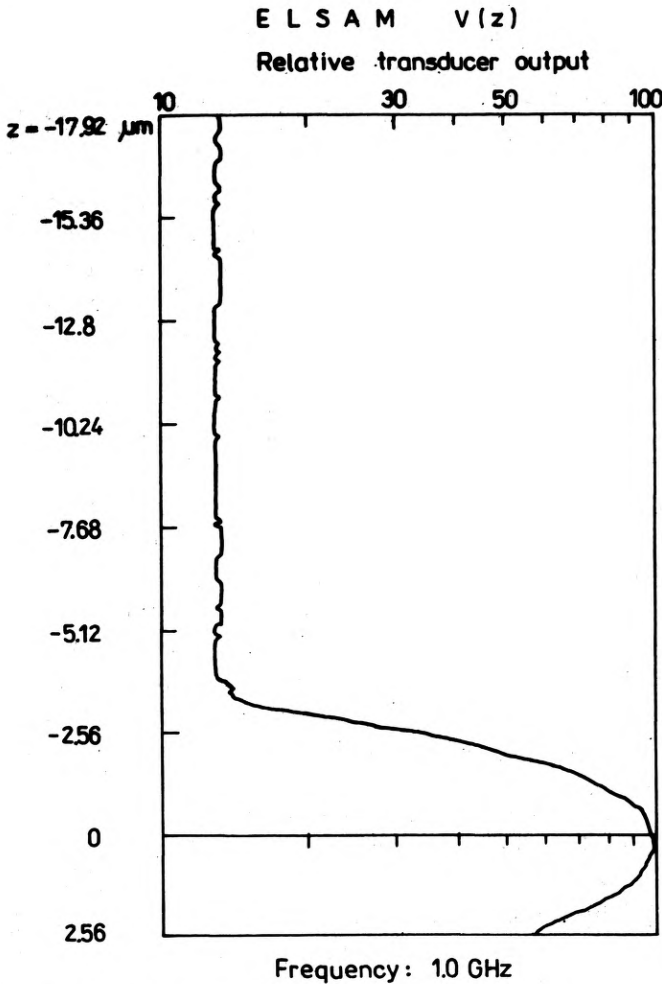


Fig. 3.  $V(z)$  function for the optical glass SF-5, the surface waves are not excited

#### 4.2. SAM as a interference microscope

As it was mentioned above, when the ultrasonic surface waves are generated, it is possible to consider SAM as an interference microscope (Fig. 5), where the reference beam is the beam  $a$  specularly reflected from the material surface. The object beam  $b$  falls on the specimen surface at the critical angle, being then transformed to the surface wave and owing to reradiation comes back to the transducer. Because of the travel along the specimen surface, this beam contains information about the passed element of the surface layer of the thickness equal approximately to one surface wavelength. When the surface waves are excited, the SAM works in interference mode and the second kind of the phase contrast appears, which is characteristic of all interference microscopes and the three kinds of contrast overlap: the amplitude caused by alternation of the modulus of the reflectance function; phase I caused by the alternation of the phase of the reflectance functions and phase II (interferometric)

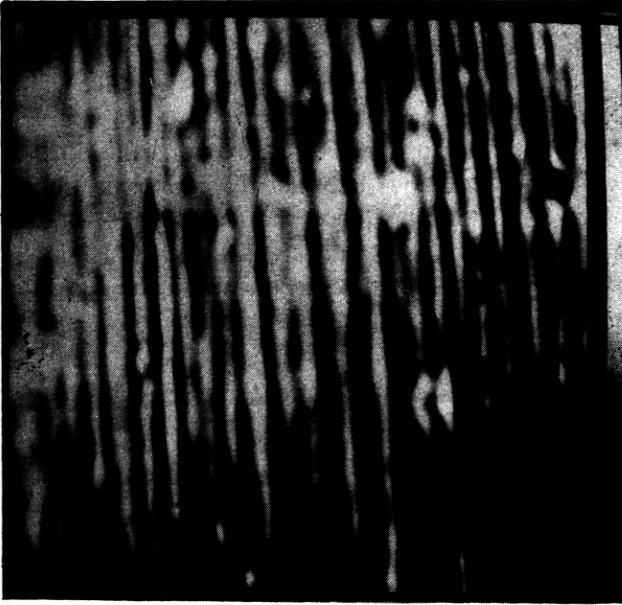


Fig. 4. Gold surface polished with 3  $\mu\text{m}$  diamond paste (magnification 425  $\times$ )

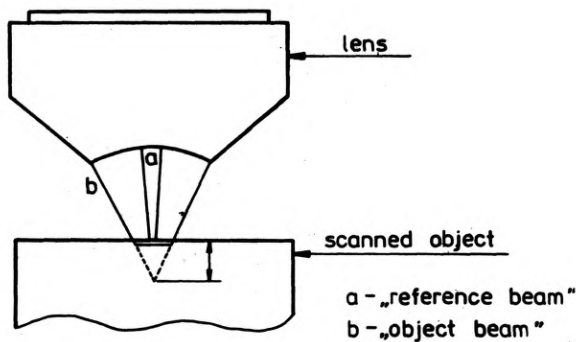


Fig. 5. Interference phenomena in the SAM

caused by alternation of surface waves velocities. The resultant contrast is affected also by the attenuation of the surface wave. The amplitude contrast is in most cases weak. It is, therefore, possible to assume that when SAM is defocused, both phase contrasts I and II play predominant role. It should be underlined that both of them are directly connected and the classification introduced (based on [25]) has only an intuitive meaning. It is possible, of course, to treat both phase contrasts as a single one and consider only the behaviour of the reflectance function (its modulus and phase) in the whole range of the angles of incidence [26].

#### 4.3. SAM in non-scanning mode. Measurement of the $V(z)$ function

The measurement of the output signal of the transducer, i. e., the  $V(z)$  function, is the

next important application of the SAM. There are two approaches to theoretical evaluation of this function. The first one [26], derived from Fourier optics, considers behaviour of an angular spectrum of the ultrasonic wave generated by transducer, its diffraction on the acoustic lens and reflection from the specimen surface. The returning signal in the plane of the transducer is synthesized from its angular spectrum. The second one, i.e., the ray optical approach [25], explains the output signal from the transducer as a result of interference between the beam specularly reflected from the investigated surface and the other one reradiated by the surface wave into the liquid. The angle of reradiation is equal to the critical angle (Snell law). The  $V(z)$  function depends on both the properties of the specimen and the acoustic lens [27] in the following way:

$$V(z) = 2\pi \int_0^{f \sin(\alpha)} U(r)^2 P(r)^2 R(r/f) \exp[2k_0 z (1 - (r/f)^2)^{0.5}] r dr.$$

This can be recognized as a Fourier transform

$$V(z) = \exp(j4\pi z) F \left\{ \Pi \left[ \frac{t}{4 \sin^2(\alpha/2)} - \frac{1}{2} \right] U^2(t) P^2(t) R(t) \left( 1 - \frac{1}{2} t \right) \right\}$$

where:  $t = 2[1 - (1 - (r/f)^2)^{0.5}]$ ,

$P^2(t)$  – pupil function of the acoustic lens (it was assumed that  $P_1 = P_2 = P = P^*$ ),

$U^2(t)$  – pupil function of the transducer (in both directions),

$R(t)$  – reflectance function of the specimen.

It is easy to notice that for a given lens the functions  $U^2(t)$  and  $P^2(t)$  are known, and the  $V(z)$  function is completely determined by elastic properties of the specimen, i.e., its reflectance function  $R(t)$ . The rapid phase change of  $R(t)$  (about  $2\pi$ ) occurs at the angle at which coupling between the longitudinal wave in fluid and the surface wave takes place. This change is responsible for oscillation in  $V(z)$  function. It also appears as a lateral Schoch displacement [28] in the course of reflection of a bounded acoustic beam. This displacement can be also explained as a result of excitation of the surface waves and was visualized by Schlieren photographs [29], [30]. This phenomenon is analogous to the Goos–Hänchen shift in optical case [31]. The surface waves propagating along the specimen surface are attenuated. Beside the phase information about ultrasonic path passed, the waves reradiated by this surface wave carry also the amplitude information about attenuation occurring in the course of propagation on the specimen surface. If one can well separate those pieces of information, it will be possible to apply the SAM to the surface quality investigation. There were some attempts to measure the attenuation coefficient of the surface waves by the SAM [13], [16], [32]. KUSHIBIKI [12] has shown that the velocity of the surface appears in the term of modulation frequency of the  $V(z)$  function, while the attenuation coefficient appears in the expression for the depth of modulation of this function. The total attenuation coefficient of the surface wave consists of the following parts: the attenuation caused by reradiation into coupling medium, the bulk attenuation, and the attenuation caused by deficiencies of the surface layer. The

first two components can be calculated [14], [33], then, based on total attenuation coefficient measurement, it is possible to separate its part caused only by the deficiencies of the surface. The wavelength of the surface wave is about microns, but, as was shown in [15], also nanometer grain structure affects the propagating surface wave. This nanometer grain structure cannot be visible in the scanning image but it appears in the attenuation coefficient and can be detected in the non-scanning mode by  $V(z)$ -function measurement.

Recapitulating, the  $V(z)$ -function measurement gives rather full information about mechanical properties and the structure of the investigated surface on microscopic scale. The example of such function for optical glass SK-16 is given in Fig. 6, the surface waves are excited and interference oscillations in the  $V(z)$  curve are present. There is a possibility to calculate the leaky surface wave velocity  $C_s$  directly

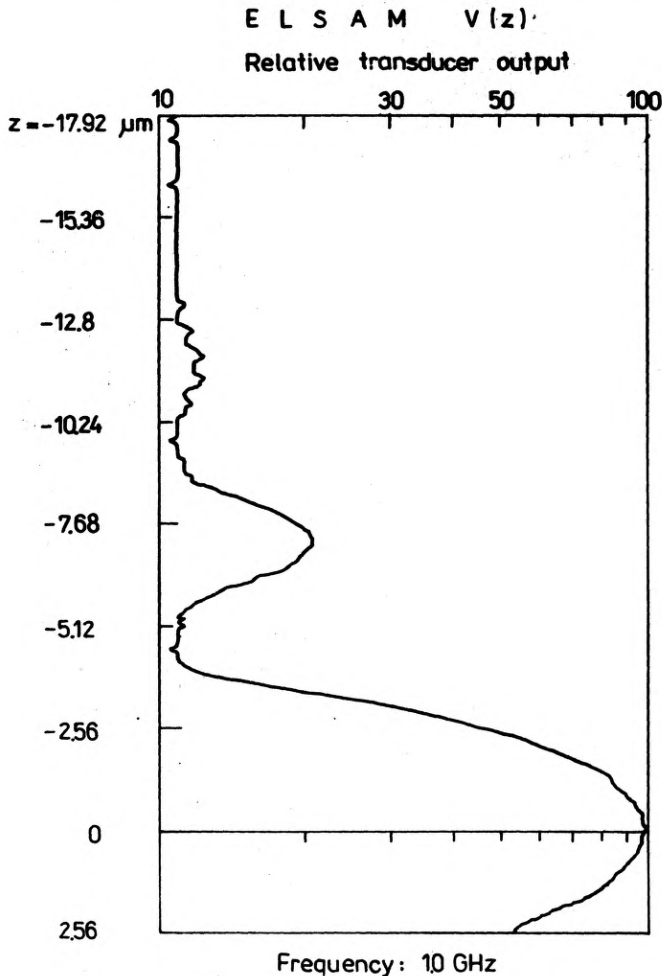


Fig. 6.  $V(z)$  function for optical glass SK-16, the surface waves are excited

from these oscillation, basing on the following formula [34]:

$$C_r = \frac{V_0}{\left[1 - \left(1 - \frac{V_0}{2fz}\right)\right]^{0.5}}$$

## 5. Investigation of optical elements

The possibility of phase imaging by SAM was utilized in investigation of optical glasses and gradient index elements. Figure 7 presents optical reflection image of the

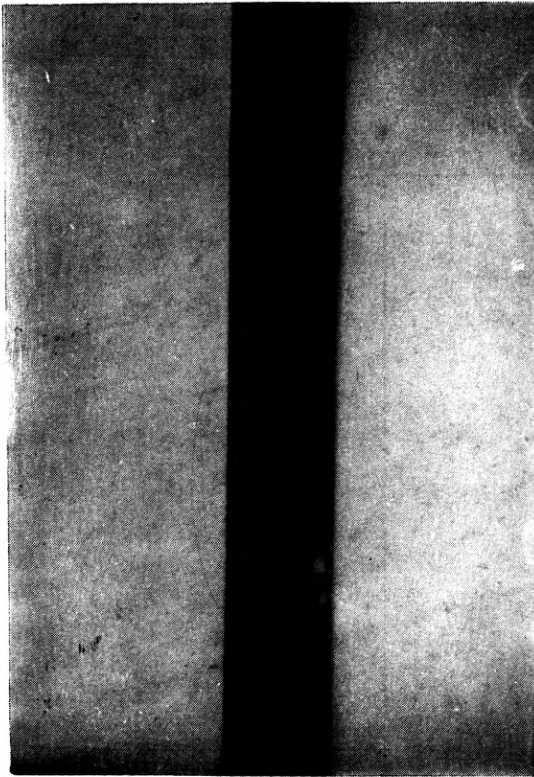


Fig. 7. Optical image of the bound between two optical glasses F-2 and SK-10 (magnification 425 ×)

boundary between two different optical glasses F2 and SK-10. There is no contrast in the optical image, difference in optical reflectance being too small. The same result is observed in ultrasonic image when the beam is focused on the specimen surface (Fig. 8a), only the boundary as a discontinuity is visible. Those glasses have different acoustical and optical properties (Tab.). Figure 8b presents the image of the same part of the specimen, but now the SAM is defocused by  $z = -2.5 \mu\text{m}$ ; the contrast in the image appears.

The next probe is the object with continuous change of optical properties instead

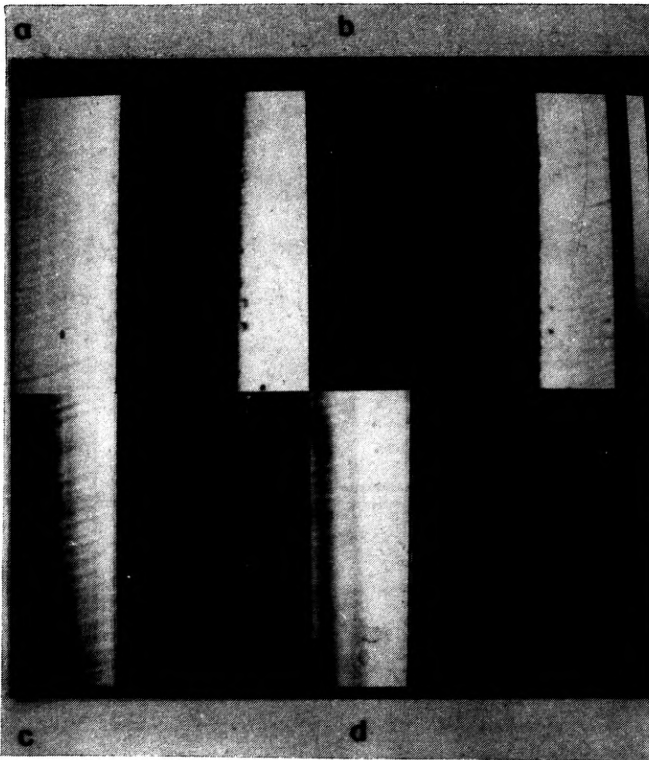


Fig. 8. Ultrasonic image of the bound between two glasses F-2 and S-10: **a** – ultrasonic focus on the glass surface, **b** – defocused image  $z = -2.5 \mu\text{m}$ , **c** –  $z = -3.50 \mu\text{m}$ , **d** –  $z = -4.20 \mu\text{m}$

Optical and mechanical parameters of the selected optical glasses [35]

Type	Optical refractive index	Abbe number	Density [kg/m <sup>3</sup> ]	Longitudinal wave speed [m/s]	Shear wave speed [m/s]	Rayleigh wave speed [m/s]
BK-7	1.51680	64.17	2510	6019	3655	3363
SK-10	1.62280	56.90	3660	5309	2966	2729
LF-6	1.56732	42.84	3110	4683	2815	2590
LaF-21	1.78831	47.39	4440	6007	3228	2970
SF-5	1.67270	32.21	4070	4004	3262	2173
SF-59	1.95250	20.36	6260	3187	1792	1649

of discontinuity as in the former experiment. This was, namely, the intersection through an optical waveguide; the intersection perpendicular to the mechanical axis of the waveguide was observed under SAM (Fig. 9). As before, the good contrast in the image is obtained after defocusing. The intensity distribution in the acoustical image of the waveguide was taken into account (Fig. 10). After certain amount of defocusing, the shape of the intensity distribution in acoustical image of the optical waveguide is similar to that for the refractive index distribution (Fig. 11). At this level of our research, it is difficult to say to what extent both distributions are the same. However, their accordance seems to be good. These results cause two questions:

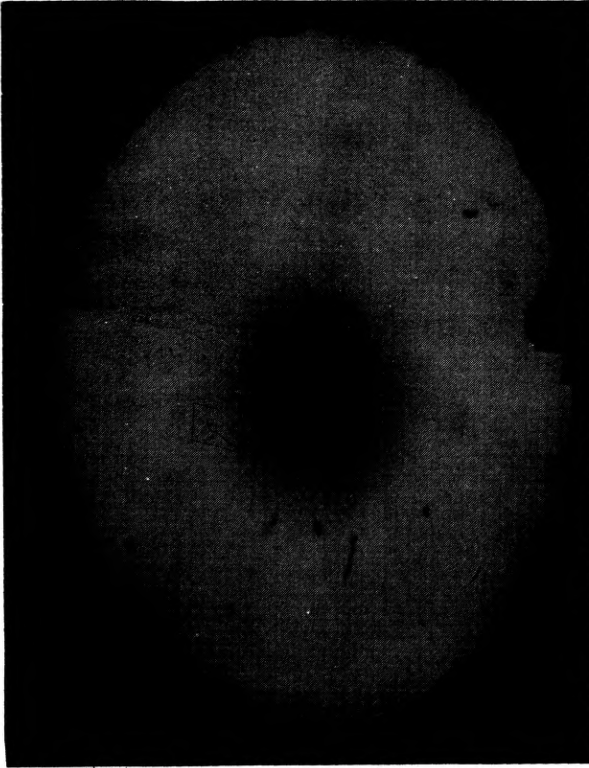


Fig. 9. Ultrasonic image of the intersection through the optical waveguide

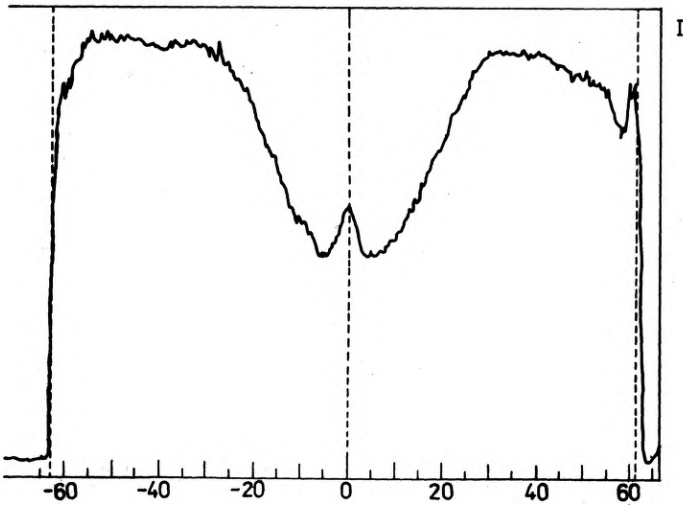


Fig. 10. Intensity distribution  $I$  in the ultrasonic image of the intersection through the optical waveguide

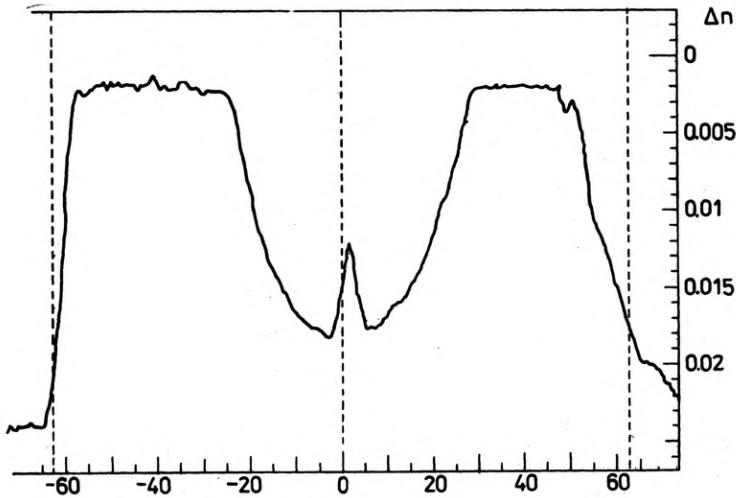


Fig. 11. Refractive index distribution  $\Delta n$  in the investigated waveguide

1. What physical value (or values) is (are) visualized by SAM?
2. What kind of relationship does take place between the values measured by SAM and optical refractive index distribution?

In order to find a correct answer to the first question, it is necessary to take into account the frequency of the ultrasound used in our experiment; it was 1.7 GHz. The resolving power at such frequency is about  $0.7 \mu\text{m}$ . The picture from SAM is the image of the acoustical properties of the specimen. They are not constant in the waveguide, as may be seen. In the case when the ultrasound beam is focused below the surface, the amount of defocusing changes from point to point (because of the difference in acoustical properties). Let  $\Delta z$  denote the maximum difference in the focus position below the surface. In the course of defocusing the value  $\Delta z$  is moved along the  $z$ -axis and the relative contrast between two different areas changes. This will be clear when we consider the sketch of the  $V(z)$  function and the sector  $\Delta z$  moving along the  $z$ -axis. The correct measurements are possible when the position of the sector  $\Delta z$  corresponds to quasi-linear part of the  $V(z)$  curve for the all the points considered, which requires a small maximum difference in surface wave velocities in the measured specimen (about hundred m/s). It is necessary to correct in this case the intensity distribution in all points of the image based on the knowledge of the  $V(z)$  function. The answer to the second question cannot be given at present. It is only possible to propose the manner of solution of this problem. From experiment, it is evident that there exists an accordance between acoustical and optical properties in the optical waveguide. It is suspected that the chemical and physical processes, which take place in the course of the waveguide manufacturing and which are responsible for final optical refractive index distribution, change also mechanical properties of the waveguide. Moreover both changes are interconnected. In order to recover these processes, it is proposed to consider in detail the technology of optical guides

manufacturing and to control the mechanical properties using the SAM after each process in the course of production.

## 6. Conclusions

When the surface acoustic waves are excited on the specimen surface by the acoustic lens, the contrast in the image is conditioned mainly by the alternation of the phase of the reflectance function (phase I contrast) and ultrasonic velocities (phase II contrast). It was observed that phase I contrast decays with defocusing and for a large amount of defocusing phase II contrast is of primary importance. This is only a qualitative evaluation, as a next step quantitative evaluation ought to be found. The shares of both kinds of contrast in the whole range of defocusing should be established exactly. It is suspected that the solution of the contrast problem is connected also with the answer to the following question: which microscope and material parameters determine the width of the zero maximum in the  $V(z)$  function, this width is different for different materials.

It was found that, in the case of optical waveguide for certain amount of defocusing, the distribution of the intensity in the ultrasonic image is similar to the distribution of the optical refractive index. This amount has been found experimentally and, as a next step, it should be found and explained theoretically. The second conclusion is that there are some technological processes which may change parallelly some optical and mechanical properties of the processed materials. After such processes the direct accordance between optical and mechanical parameters may be recovered.

The measurement of the  $V(z)$  function gives potential possibility of investigating the quality of the specimen surface layer with a rather good accuracy.

The described and applied analogy between SAM and SOM, type 2, is valid only when the SAM works in pure reflection mode, the complex amplitude detected by the transducer is switched and the illumination is harmonic. It seems very important to extend this analogy to the case when the surface waves are excited and the loss of information between the piezoelectric receiver and the monitor of the SAM takes place.

The data presented in the Table were taken from the Schott catalogue *Optical Glasses* No. 3111d [35]. This catalogue contains about 240 different types of optical glasses with different longitudinal velocity changing from 6000 down to 3000 m/s. This interval is nearly continuously filled. The optical glasses are materials of high homogeneity and their surface may be prepared with high quality. All those facts make possible application of those materials as a source of reference of the acoustical parameters. For example, applying glasses of surface wave velocity ranging in the vicinity of 3000 m/s, it is easy to verify the value of the aperture semi-angle of the ultrasonic lens. If the lens investigated with nominal aperture semi-angle of 30 deg does not excite surface waves of surface wave velocity of 3000 m/s on the specimen surface, this aperture semi-angle must be smaller than 30 deg. Such results were observed in practice. Using the set of glasses one can check this angle.

## Appendix

The critical angle is the angle at which the coupling between longitudinal wave in liquid and surface wave on the liquid-solid specimen interface takes place. When the confined ultrasonic beam falls from the liquid to the liquid-solid interface at critical angle, its energy is transformed into the surface waves. Of course, this transformation is possible and takes place either in both directions or attenuation-free on the interface, so that the excited surface wave reradiates its energy back into the liquid in the course of propagation. The term "leaky surface wave" is used to this wave. The Snell law allows reradiation only at critical angle. The phenomena of excitation and reradiation of the surface wave play fundamental role in the imaging process of SAM.

In the continuous free space without attenuation elastic waves are non-dispersive, the dispersion appears together with confinements of the region in which elastic waves propagate or when this region cannot be treated as continuous. Dispersion becomes significant when the dimension of confinements or discontinuity is comparable with wavelength [10]. This means, for example, that when the elastic wave propagates in the layer of thickness not higher than several wavelengths, the dispersion phenomenon must be taken into account. On the other hand, when the same wave propagates in the free space filled with crystal, in which the distances between crystallographical planes are comparable with the wavelength of the elastic wave, the dispersion curve may no more be approximated by a straight line and the dispersion appears again. In the case of acoustic microscopy, we work with wavelength not shorter than hundreds of nanometer. Therefore, the assumption of dispersion absence is acceptable. In the presence of absorption velocity of elastic wave becomes complex and imaginary part depends on the attenuation coefficient. This dependence can be also considered as a kind of dispersion.

*Acknowledgements* – The authors wish to thank Dr H. Kasprzak whose ideas were the basis of the experiments with optical elements, Dr E. Pawlik, for preparing the probes for experiments, Dr M. Pluta, for the measurement of the refractive index distribution in probes examined, and Doc. Dr I. Wilk, for his helpful critical remarks (all from the Technical University of Wrocław, Poland). We express our thanks to Dipl. Ing. R. Lasch and Dr H. Block from the University of Bremen, for their help in the course of experiments. The investigated optical waveguide has been made in the Optotelecommunication Center (OTO), Lublin, Poland.

## References

- [1] SHEPPARD C. J. R., CHOUDHURY A., *Opt. Acta* **24** (1977), 1051.
- [2] SHEPPARD C. J. R., WILSON T., *Opt. Acta* **25** (1978), 315.
- [3] LEMONS R. A., QUATE C. F., *Physical Acoustic*, [Ed.] W. P. Mason, Academic Press, New York, London 1979, Vol. 14.
- [4] SOMEKH M., BRIGGS G., ILETT Ch., *Philos. Mag. A* **49** (1984), 179.
- [5] WEAVER J., SOMEKH M., BRIGGS G., PECK S., ILETT Ch., *IEEE Trans. Sonics Ultrasonics* **32** (1985), 302.
- [6] ISHIKAWA I., SEMBA T., KANDA H., KATAKURA K., TANI Y., SATO H., *IEEE Trans. Ultrasonics, Ferroelectrics, Frequency Control* **36** (1989), 274.
- [7] FOSTER J., RUGAR D., *IEEE Trans. Sonics Ultrasonics* **32** (1985), 139.

- [8] HADIMIOGLU B., FOSTER J., *J. Appl. Phys.* **56** (1984), 1976.
- [9] QUATE C. F., *IEEE Trans. Sonics Ultrasonics* **32** (1985), 132.
- [10] DIEULESAINT E., ROYER D., *Elastic Waves in Solids*, J. Wiley, New York 1980, pp. 21–26.
- [11] FRIGHT W., BATES R., ROWE J., SPENCER D., *J. Microsc.* **153** (1989), 103.
- [12] KUSHIBIKI J., OHKUBO A., CHUBACHI N., *Electron. Lett.* **18** (1982), 668.
- [13] YAMANAKA K., *Electron. Lett.* **18** (1982), 587.
- [14] VIKTOROW A., *Rayleigh and Lamb Waves*, Plenum Press, New York 1967, pp. 25–40, 57–68.
- [15] MORSCH A., KORN D., GLEITER H., HOPPE M., ARNOLD W., *4th Int. Conf. Materials Characteristic*, Saarbrücken 1988.
- [16] KUSHIBIKI J., CHUBACHI N., *IEEE Trans. Sonics Ultrasonics* **32** (1985), 189.
- [17] KUSHIBIKI J., MAEHARA H., CHUBACHI N., *Electron. Lett.* **18** (1981), 322.
- [18] VETTERS H., MAYR P., BOSECK S., LUEBBEN Th., MATTHAEI R., SCHULZ A., *Scanning Electron Microscopy*, SEM Inc., AMF O'Hare, Chicago 1985, III, pp. 981–989.
- [19] SHEPPARD C. J. R., WILSON T., *Optik* **55** (1980), 331.
- [20] SHEPPARD C. J. R., WILSON T., *Philos. Trans. Roy. Soc. A* **295** (1980), 513.
- [21] SHEPPARD C. J. R., WILSON T., *Appl. Opt.* **18** (1979), 1058.
- [22] SHEPPARD C. J. R., WILSON T., *Opt. Lett.* **3** (1978), 115.
- [23] GOODMAN J., *Introduction to Fourier Optics*, McGraw-Hill, San Francisco 1968, pp. 21–25.
- [24] BLOCK H., Private information (unpublished).
- [25] BERTONI H. L., *IEEE Trans. Sonics Ultrasonics* **31** (1984), 105.
- [26] ATALAR A., *J. Appl. Phys.* **49** (1978), 5130.
- [27] HILDEBRAND I. A., LIANG K., BENNETT S. D., *J. Appl. Phys.* **54** (1983), 7106.
- [28] SCHOCH A., *Acustica* **2** (1952), 18.
- [29] NEUBAUER W. G., *J. Appl. Phys.* **44** (1973), 48.
- [30] NEUBAUER W. G., DRAGONETTE L. R., *J. Appl. Phys.* **45** (1974), 618.
- [31] MCGUIRK M., CARNIGLIA C. K., *J. Opt. Soc. Am.* **67** (1977), 103.
- [32] SMITH J. R., WICKRAMASINGHE H. K., *Electron. Lett.* **18** (1982), 955.
- [33] KINO G. S., *Acoustic Waves Devices, Imaging and Analog Signal Processing*, Prentice-Hall Inc., New Jersey 1987, pp. 131–150.
- [34] WEGLEIN R. D., *IEEE Trans. Sonics Ultrasonics* **32** (1985), 225.
- [35] Schott Catalogue *Optical Glasses*, No. 3111d.

*Received May 16, 1990*  
*in revised form November 5, 1990*

### **Акустика сканирующего микроскопа. Некоторая возможность применения в исследованиях оптических стекол и волокон**

Дана краткая теория процесса отображения в акустическом сканирующем микроскопе (SAM) по отношению к оптическому сканирующему микроскопу (SOM) типа 2. При некоторых условиях SAM работает похоже на SOM типа 2, но он может использовать также явление интерференции в процессе отображения. SAM очень чувствителен к топографии поверхности и хорошего контраста образа можно достичь также тогда, когда явление интерференции не выступает. Даны результаты измерений оптических стекол и световодов, которые ведут к выводу, что технологический процесс, примененный в изготовлении световодов изменяет параллельно оптические и механические свойства обрабатываемого материала.

*Перевел Станислав Ганцаж*